Journal of Medicinal Chemistry

Article

pubs.acs.org/jmc

Inhibitors of Human Immunodeficiency Virus Type 1 (HIV-1) Attachment 13. Synthesis and Profiling of a Novel Amminium Prodrug of the HIV-1 Attachment Inhibitor BMS-585248

Alicia Regueiro-Ren,*[,†] Jean Simmermacher-Mayer,[‡] Michael Sinz,*[,‡] Kim A. Johnson,[‡] Xiaohua Stella Huang,[‡] Susan Jenkins,[‡] Dawn Parker,[‡] Sandhya Rahematpura,[‡] Ming Zheng,[‡] Nicholas A. Meanwell,[†] and John F. Kadow[†]

[†]Departments of Medicinal Chemistry and [‡]Pharmaceutical Candidate Optimization, Bristol-Myers Squibb Research and Development, 5 Research Parkway, Wallingford, Connecticut 06492, United States

ABSTRACT: In vitro studies suggested that the ammonium salt **2** could be a viable prodrug of the HIV-1 attachment inhibitor **1**. Increased systemic exposure of the parent drug **1** following oral administration of the amminium salt **2** when compared to similar studies using solution dosing of the parent compound was observed in the in vivo studies in both rats and dogs. At high doses, the improvement in oral exposure of the parent drug was even more evident, indicating that the increased solubility of the amminium salt **2** can overcome dissolution-limited absorption and demonstrating the potential utility of this compound as a prodrug of **1**.

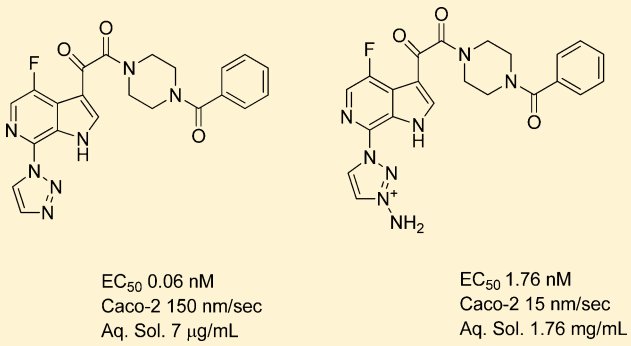

INTRODUCTION

BMS-585248 (**1**), a potent, third-generation HIV-1 attachment inhibitor (AI) with a promising initial in vitro and in vivo pharmacokinetic profile, was selected for preclinical evaluation in higher species and eventually as a candidate for clinical development.[1] However, at high doses, **1** displayed poor oral exposure which was attributed to poor solubility (7 μg/mL) and, as a result, its development presented a challenge. Several strategies were explored in order to improve the exposure of **1**. Among them were alternative formulations and the use of classical prodrugs such as phosphate-based approaches which had proved successful with previous compounds in this class.[2] In a parallel approach, we focused on introducing polar or ionizable substituents onto **1** in an effort to increase solubility and thus overcome the dissolution-limited absorption. Installation of an amino moiety in the pyridyl group was considered as both a means of introducing a charge into the structure as well as a handle for further elaboration. However, when **1** was submitted to amination conditions, the amino group was introduced to the triazole moiety rather than the pyridine to afford the novel *N*-amino-triazolium (amminium) salt **2** (Figure 1).[3,4]

Amminium salt **2** displayed improved aqueous solubility (1.76 mg/mL) but poor antiviral potency (EC_{50} = 1.76 nM) and considerably decreased membrane permeability when compared with **1** (15 nm/s vs 150 nm/s in the Caco-2 assay). On the basis of this profile, **2** did not appear to have potential to be a useful antiviral agent and we were unaware of examples in the literature where amminium salts served as viable prodrugs. However, it is known that N-oxides can act as prodrugs by releasing the parent drug in vivo via reductive cleavage of the N−O bond.[5,6] We

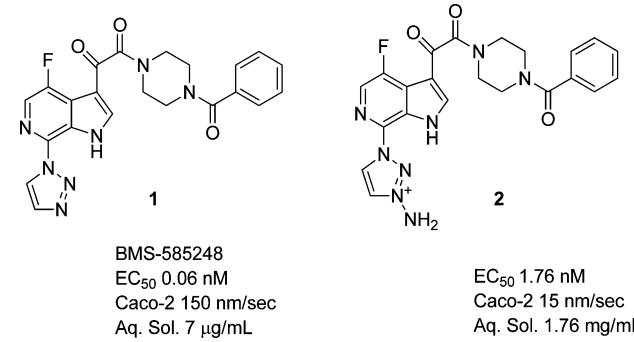

Figure 1. BMS-585248 (**1**) and its amminium prodrug (**2**).

hypothesized that the N−N bond in **2** could be susceptible to a similar cleavage, resulting in the release of the parent drug **1**. Preliminary in vitro experiments demonstrated that conversion to the parent was possible. Subsequently, increased systemic exposure of the parent drug **1** following oral administration of the amminium salt **2** when compared to similar studies using solution dosing of the parent compound was observed in both rats and dogs. At high doses, the improvement in oral exposure of parent drug was even more evident, indicating that the increased solubility of the amminium salt **2** can overcome the dissolution-limited absorption and demonstrating the potential utility of this compound as a prodrug. Several other experiments helped determine the mechanism by which the parent drug is released as

Received: November 6, 2012
Published: February 1, 2013

dx.doi.org/10.1021/jm301638a | *J. Med. Chem.* 2013, 56, 1670−1676

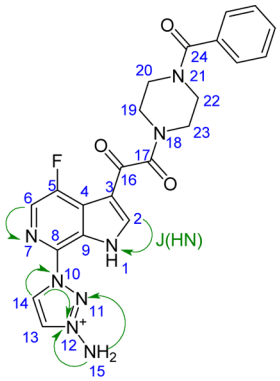

Atom #	N1	N7	N10	N11	N12	N15
chem shift	153.5	276.9	240.2	324.8	265.1	102.1

Figure 2. Nitrogen chemical shift assignment for **2**. The ^{15}N chemical shifts were referenced to NH_3 (liq) at −380.2 ppm..

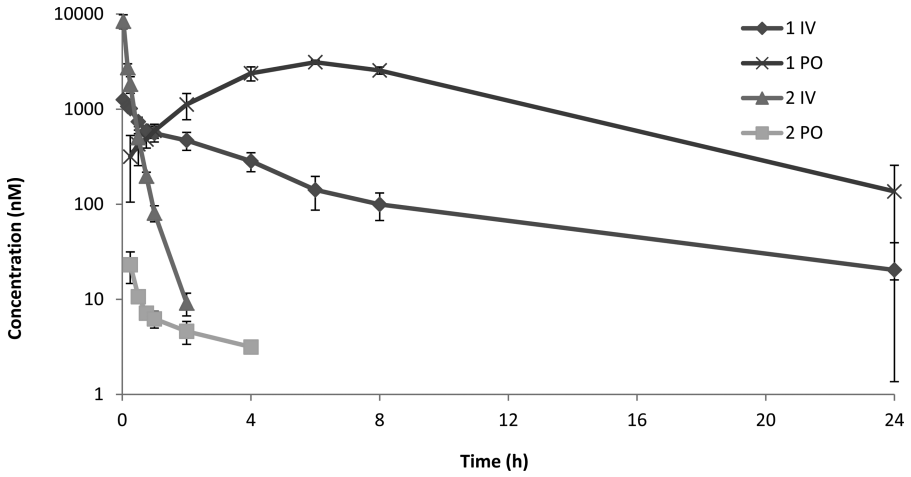

Figure 3. Rat plasma concentration−time profiles of **1** and **2** after intravenous (1 mg/kg) and oral (5 mg/kg) dosing of **2** (mean ± SD).

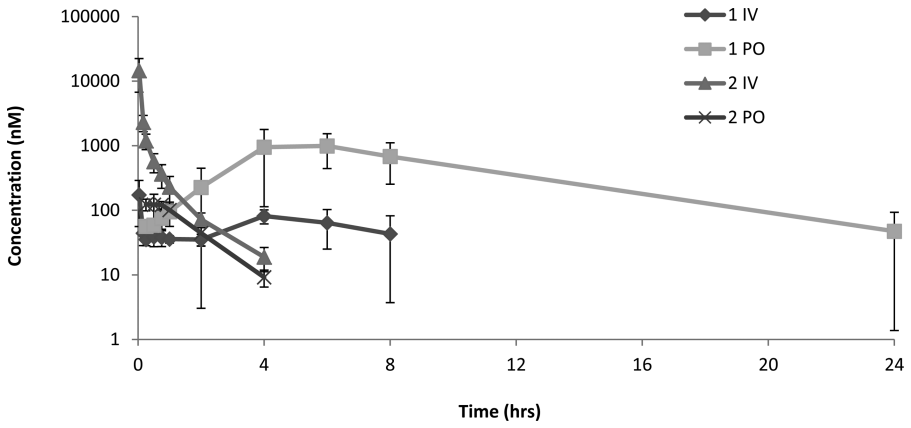

Figure 4. Dog plasma concentration−time profiles of **1** and **2** after intravenous (1 mg/kg) and oral (5 mg/kg) dosing of **2** (mean ± SD).

well as illustrate the potential to apply this methodology to other unrelated chemotypes.

CHEMISTRY

The conversion of **1** into amino salt **2** was accomplished in 25% yield by regioselective amination of **1** using a methylene chloride solution of NH_2OTs[7] at ambient temperature. Other amination methods, i.e., hydroxylamine-*O*-sulfonic acid;[8] *O*-(2,4-dinitrophenyl) hydroxylamine[9] rendered no desired product, which seemed most likely due to the poor solubility of **1** in the reaction media. The resulting amminium tosylate salt was converted into the amminium chloride salt by chromatography using an ion exchange column. All in vitro and in vivo experiments were performed using the chloride salt. The connection between the

dx.doi.org/10.1021/jm301638a | J. Med. Chem. 2013, 56, 1670−1676

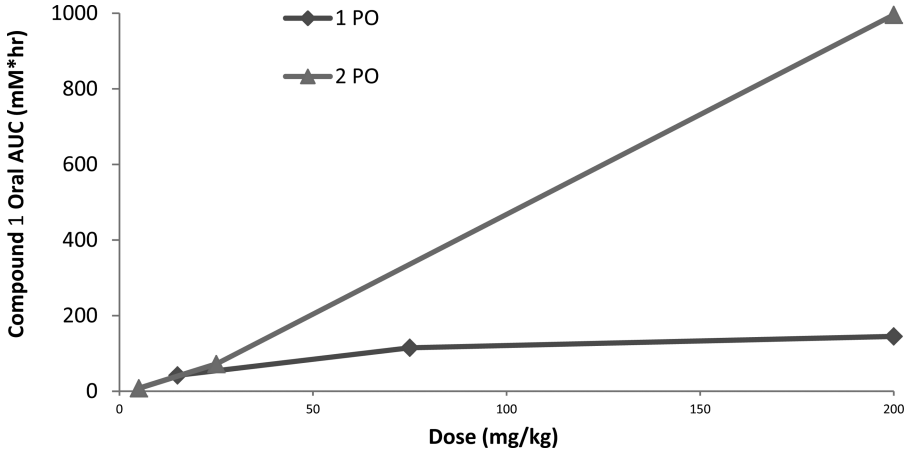

Figure 5. Rat dose escalation study after oral dosing of **2** (prodrug) and **1**.

amino group (NH_2) and the triazole N12 nitrogen was confirmed by the observation of the H−N long-range correlation between the amino proton H15 (9.06 ppm) and the N12 nitrogen (265.1 ppm) (Figure 2). This conclusion is further supported by the NOE observed between the N15 proton and H13 (9.01 ppm).

RESULTS AND DISCUSSION

In Vivo Conversion of 2 in Rats and Dogs. Conversion of the prodrug **2** to the parent **1** was observed following both intravenous (IV) and oral (PO) administration in rats. The plasma profiles obtained from the pharmacokinetic experiments are shown in Figure 3. Following IV administration of **2** to male rats, the prodrug had a moderate clearance (23 mL/min/kg), a low volume of distribution (0.29 L/kg), and a short half-life (0.3 h). The conversion of prodrug was rapid after IV dosing with **1** appearing at the earliest time point (5 min). Following IV administration of **2**, **1** had 2-fold higher AUC than **2** (3220 vs 1553 nM·h, respectively). Following oral administration of **2**, very low exposure of the prodrug was observed, with a C_{max} of 23 nM while relatively high exposure of **1** was observed, with a C_{max} of 3121 nM 6 h postdose. The exposure of **1** was much greater than **2** after oral dosing (28098 vs 20.8 nM·h, respectively), indicating substantial conversion of the parent drug from the prodrug. Similar increases in systemic exposure of the parent drug following administration of prodrug were also observed in male beagle dogs (Figure 4). Following IV administration of **2** at **1** mg/kg, moderate clearance (13.8 mL/min/kg), a low volume of distribution (0.3 L/kg), and a short half-life of 2 (0.9 h) were observed. Conversion to **1** after IV adminstration occurred with an AUC **1**/AUC **2** of ∼16%. Following oral administration of **2** in dogs, low exposure of the prodrug was observed (C_{max}: 139 nM); however, the exposure of the parent was ∼8-fold higher. The exposure of **1** was again much greater than **2** after oral dosing (8064 vs 217 nM·h, respectively). These data in rats and dogs indicate that the prodrug **2** is rapidly and extensively converted to the parent drug **1** in vivo.

In a rat dose escalation study, **2** and **1** were dosed orally at 5, 25, and 200 mg/kg and 5, 15, and 200 mg/kg, respectively. Dose-limiting absorption was observed after administration of **1** at higher doses of 75 and 200 doses mg/kg, as would be expected for a poorly soluble compound. However, dose-proportional increases in C_{max} and greater than dose-proportional increases in AUC of parent drug **1** were observed following administration of the prodrug up to 200 mg/kg (Figure 5, Table 1).

Table 1. Pharmacokinetic Parameters from Rat Dose Escalation Study

parameter	2			1		
dose (mg/kg)	5	25	200	15	75	200
C_{max} (μM)	1.3	12	77	6.6	8.4	11
AUC_{tot} (μM·h)	8	72	996	42	115	145

In Vitro Conversion of 2. With in vivo rat and dog pharmacokinetic studies showing markedly increased systemic exposure of the parent after administration of the amminium prodrug, further in vitro and in vivo experiments were conducted in order to investigate the mechanism by which the prodrug is converted to parent drug in intact animals. Despite rapid and extensive conversion in vivo, **2** was found to be stable in Tris-HCl buffer (pH 7.4), rat blood, rat plasma, rat liver cytosol, microsomes, and hepatocytes when the compound was incubated under conventional aerobic conditions. Typically microsomal enzymes oxidize compounds, however, they also have the ability to reduce compounds and this reduction can be enhanced under anaerobic incubation conditions.[10] Low amounts of conversion of prodrug to parent were observed in rat and human liver microsomes when incubated under anaerobic conditions (∼10% and 4%, respectively). Additional incubations using recombinant CYPs under anaerobic conditions indicated CYP3A4 and CYP2D6 have the ability to convert prodrug to parent, however, the amounts formed were too low to accurately quantify.

Contribution of Gut Metabolism in the Conversion of 2. Because the cleavage occurred under reducing conditions in vitro, additional in vivo experiments were conducted to determine if the reductive metabolism was mediated by the liver or microflora present in the gastrointestinal tract. To assess the effect of intestinal microflora on metabolism, an antibiotic-treated rat model was used. Figure 6 shows the pharmacokinetic profiles of both prodrug **2** and parent **1** after oral administration of **2**. The exposure (AUC and C_{max}) of **1** following administration of **2** to antibiotic-treated rats decreased 3.5-fold and 5.6-fold, respectively, when compared to vehicle-treated animals (Table 2). However, pretreatment of rats with antibiotics did not alter the systemic exposure of **2** following an oral dose of **2**. These data indicate that removal of the anearobic bacteria responsible for gut reductive metabolism has an impact on the formation of **1** (significantly lower parent drug), yet has only a minor effect on

dx.doi.org/10.1021/jm301638a | J. Med. Chem. 2013, 56, 1670−1676

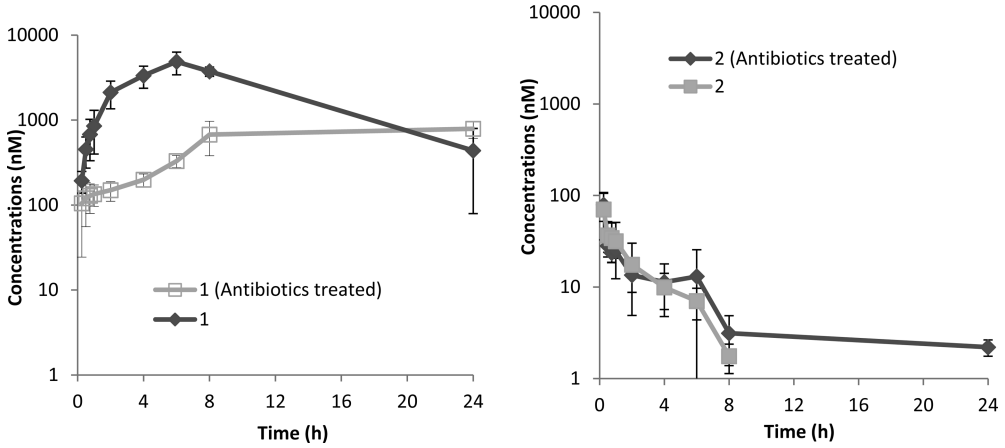

Figure 6. Exposure profiles of **1** and **2** after oral dosing of **2** (5 mg/kg) in antibiotic treated animals. Each data point is expressed as mean ± SD.

Table 2. Pharmacokinetic Parameters from Rats Pretreated with an Antibiotic

parameter	2		1	
treatment	+ antibiotics	− antibiotics	+ antibiotics	− antibiotics
C_{max} (nM)	79	70	18	7
AUC_{last} (nM·h)	148	112	13761	47535

the exposure of the prodrug **2** (minor increases in the exposure of **2**).

Because both gut microflora and hepatic enzymes (CYP2D6 and CYP3A4) appeared to mediate the reductive metabolism of **2**, the relative contribution of hepatic vs gut metabolism in the conversion of **2** was evaluated using dual cannulated portal vein and jugular vein rats. Following oral administration of the prodrug **2**, the concentration vs time profiles of both the prodrug and the parent in the portal vein (prehepatic) were similar to the respective profiles in the jugular vein (posthepatic) samples. Overall, very low levels of **2** (74 nM and 35 nM·h, C_{max} and AUC (portal vein), respectively) were observed in both portal and jugular vein samples and the majority of drug-related material was parent drug (2137 nM and 23873 nM·h, C_{max} and AUC (portal vein), respectively) (jugular vein data not shown). These data suggest that the majority of the prodrug conversion occurs at the level of the intestine

To further evaluate the metabolite disposition of the prodrug, a biotransformation study was conducted using bile duct cannulated rats (Scheme 1). Relative percentages of **2**, an *N*-acetyl conjugate **3**, and **1** in plasma were 68%, 15.7%, and 16%, respectively (pooled plasma from 0 to 2 h post dose). The major drug-related components observed in bile were the *N*-acetyl conjugate **3** and **2**, with a metabolite-to-prodrug ratio of 9:1,

Scheme 1. Metabolites of 2 Observed in Bile Duct Cannulated Rats

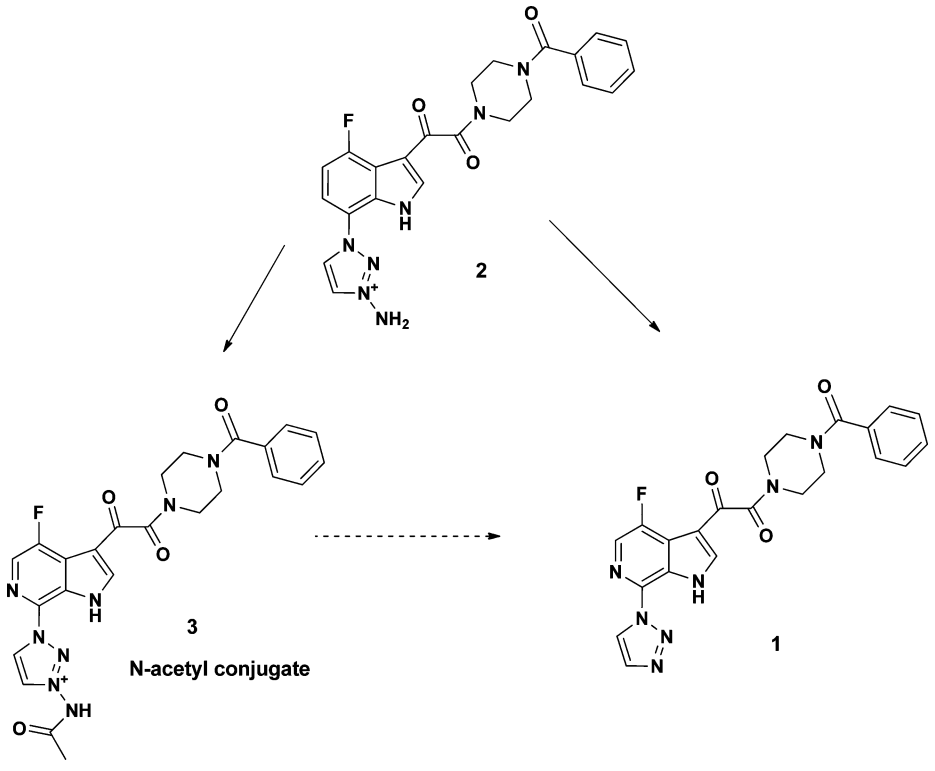

dx.doi.org/10.1021/jm301638a | J. Med. Chem. 2013, 56, 1670−1676

while **1** was not observed in bile. In addition to **2**, both the *N*-acetyl conjugates **3** and **1** were detected in urine at relative percentages of 80%, 16.5% ,and 3.5%, respectively.

High-Throughput in Vitro Method for the Screening of Amminium Prodrug. To investigate the utility of this prodrug with other *N*-amino compounds, as well as to develop a higher throughput method to assess the participation of intestinal microflora in the metabolism of this type of prodrug, **2** was incubated in fresh rat fecal homogenate. After a 2 h incubation, a 96% conversion of prodrug **2** to parent **1** was observed. This same in vitro method was used with several other N-aminated heterocycles (**4** and **5**) (Figure 7), each of which showed conversion to parent compound (**4**, 88%, and **5**, 35% conversion).

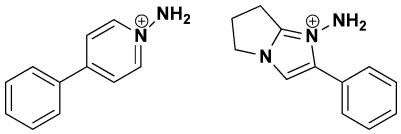

4 5

Figure 7. Model N-aminated heterocycles **4** and **5**.

CONCLUSION

An amminium salt **2** of the 1,2,3-triazole-containing HIV-1 attachment inhibitor **1** was found to behave as a prodrug, showing good systemic exposure of the parent **1** following oral administration to both rats and dogs. The improved solubility of the amminium prodrug allowed for higher doses to be administered and overcame the solubility-limited absorption associated with the parent drug. In principle, any compound with a nitrogen-containing heterocycle can be aminated and the amminium salt, providing that it is chemically stable, could be used as a potential prodrug. This approach provides a potentially useful method to help with the progression in the clinic and further development of BCS class 2 compounds,[11,12] where this structural modification can be introduced. The in vitro and in vivo experiments indicate that the amminium salt is predominately cleaved presystemically by the gut microflora to release the parent compound **1**, which is highly permeable and readily absorbed. An in vitro assay using rat feces, which are rich in gut microflora, was developed and used to find that the amminium salt of pyridines and imidazoles are converted efficiently to the parent compound, demonstrating broader applicability of the prodrug technology. Although gut physiology and diet will influence the microflora between animals and humans in rate and extent of reduction, the reductive cleavage reaction should nonetheless occur to some extent across all species.[13] Some variation in the gut microflora across the human population is also anticipated; however, the differences are not expected to be dramatic. However, gut microflora can be sensitive to antibiotics and patients undergoing treatment with an antibiotic may have significantly different levels/types of intestinal flora. This can precipitate a drug−drug interaction in which the antibiotic therapy would reduce the efficiency of the prodrug release from an amminium species. This is an aspect of this prodrug technology that requires further consideration and evaluation.

EXPERIMENTAL SECTION

Chemistry. All commercial reagents and anhydrous solvents were purchased from commercial sources and were used without further purification or distillation, unless otherwise noted. Analytical high pressure liquid chromatography (HPLC) and LC-MS analyses were conducted using Shimadzu LC-10AS pumps and a SPD-10AV UV−vis detector set at 254 nm with the MS detection performed with a Micromass Platform LC spectrometer for LC in electrospray mode. NMR (^{1}H, ^{13}C, and ^{15}N) spectra were recorded on a Bruker 500 MHz spectrometer equipped with a 5 mm TCI cryo probe in DMSO. The proton and carbon chemical shift were referenced to TMS at 0.00 and are reported in ppm. The nitrogen chemical shift was referenced to liquid NH_3 at −380.2 ppm. High-resolution mass spectra (HMRS) were recorded on an LTQ-Orbitrap.

1-Amino-3-{3-[2-(4-benzoyl-piperazin-1-yl)-2-oxo-acetyl]-4-fluoro-1*H*-pyrrolo[2,3-*c*]pyridin-7-yl}-3*H*-[1,2,3]triazol-1-ium. A cloudy semisolution of 1-(4-benzoyl-piperazin-1-yl)-2-(4-fluoro-7-[1,2,3]triazol-1-yl-1*H*-pyrrolo[2,3-*c*]pyridin-3-yl)-ethane-1,2-dione[1] (160 mg, 0.35 mmol) in CH_2Cl_2 was treated with 5 mL of a CH_2Cl_2 solution of H_2NOTs (prepared as indicated below) and stirred at rt for 3 h, at which point the reaction had become homogeneous. The solvent was removed in vacuo, and the residue was dissolved in MeOH and purified using a medium pressure reverse phase column (YMC C18) and 10% MeCN/99% H_2O/1% HCl to 50% MeCN/49% H_2O/1% HCl as the mobile phase to afford the chloride salt of compound **2** as a pale-yellow solid (40 mg, 23%). Analytical RP-HPLC t_R = 6.70 min (Sunfire C18 3.5 μm, 3.0 mm × 150 mm, 15 min gradient, 1 mL/ming, 9.5% MeCN/H_2O/0.1%TFA to 95% MeCN/H_2O/0.1%TFA, 254 nm, purity 99.1%). HRMS *m/z*: (M^+) calcd for $C_{22}H_{20}O_3N_8F$, 463.1637; found, 463.1623. ^{1}H NMR (500 MHz, DMSO-d_6) δ 13.63 (br s, 1H), 9.55 (br s, 1H), 9.06 (br s, 2H), 9.01 (br s, 1H), 8.65 (s, 1H), 8.44 (s, 1H), 7.45 (br s, 5H), 3.69 (br s, 4H), 3.49 (br s, 4H). ^{13}C NMR (126 MHz, DMSO-d_6) δ 184.0, 169.3, 165.4, 153.6 (d, J = 263.4 Hz), 142.5, 135.5, 126.5 (d, J = 29.1 Hz), 126.7, 122.2 (d, J = 20.9 Hz), 113.4, 45.3, 40.8.

The trifluoroacetate salt of compound **2** was obtained by purification of the crude reaction productusing reverse phase HPLC (YMC C18 S5 20 × 50 mm column) and 10% MeOH/90% H_2O/0.1% TFA to 90% MeOH/10% H_2O/0.1% TFA as the mobile phase.

1-Amino-2-phenyl-6,7-dihydro-5*H*-pyrrolo[1,2-*a*]imidazol-1-ium 4-methylbenzenesulfonate (4). Prepared from 2-phenyl-6,7-dihydro-5*H*-pyrrolo[1,2-*a*]imidazole[14] following the procedure described above (white solid, 62% yield). Analytical RP-HPLC t_R = 10.38 min (Xbridge Phenyl 3.5 μm, 3.0 mm × 150 mm, 15 min gradient, 1 mL/min, 9.5% MeCN/H_2O/0.1%TFA to 95% MeCN/H_2O/0.1% TFA, 254 nm, purity 95.4%). MS: (ES^+) *m/z* $(M)^+$ = 200.14. ^{1}H NMR (500 MHz, DMSO-d_6) δ 7.86 (s, 1H), 7.79−7.69 (m, 2H), 7.59−7.50 (m, 3H), 7.47 (*d*, J = 7.9 Hz, 2H), 7.11 (d, J = 7.9 Hz), 6.60 (s, 2H), 4.27 (t, J = 7.3 Hz, 2H), 3.21 (t, J = 7.6 Hz, 2H), 2.66 (quin, J = 7.5 Hz, 2H), 2.29 (s, 3H). ^{13}C NMR (126 MHz, DMSO-d_6) δ 153.1, 145.7, 137.7, 137.6, 129.5, 128.8, 128.5, 128.1, 126.2, 125.5, 113.9, 48.7, 24.8, 23.2, 20.8. ^{15}N NMR (DMSO-d_6) δ 182.3, 175.5, 71.6.

Preparation of H_2NOTs.[7] Tosyl chloride (2.1 g, 11.0 mmol) was added in portions to a solution of ethyl *N*-hydroxyacetimidate (1.2 g, 11.6 mmol) and triethylamine (8.88 mL, 63.7 mmol) in anhydrous DMF (20 mL) at 0 °C. After addition was completed, the mixture was placed at room temperature and stirred for 1 h. The reaction mixture was poured over ice−water (100 mL) and stirred for 10 min. A white-yellowish solid was formed and collected by filtration. The solid was washed with water (3 × 50 mL) (1.3 g of the solid was collected). LC/MS: (ES^+) *m/z* $(M + 1)^+$ = 258. t_R = 1.52 min. This solid was treated with 70% $HClO_4$ (5 mL) and stirred at rt for 10 min, then in a water bath at 60 °C for 1 min and again at room temperature for 20 min. H_2O (100 mL) was added, and the reaction was extracted with CH_2Cl_2 (50 mL). The organic layer was washed with H_2O (50 mL), dried over sodium sulfate, filtered, and used as-is.

Metabolics and Pharmacokinetics. Human and rat liver microsomes, rat liver cytosol, human recombinant CYP's, and rat CYP450 reductase were purchased from BD Gentest (Woburn, MA). Rat hepatocytes were isolated and prepared at Bristol-Myers Squibb (Berry et al.[15]). Solvents were purchased from Mallinckrodt Baker (Phillipsburg, NJ), and chemicals, including PEG-400, NADPH, neomycin, tetracycline HCl, and bacitracin, were obtained from Sigma-Aldrich (St. Louis, MO). LB Broth was obtained from LifeTechnologies (Grand Island, NY). All other chemicals used were

dx.doi.org/10.1021/jm301638a | J. Med. Chem. 2013, 56, 1670−1676

from commercial suppliers. Dual cannulated portal vein/jugular vein rats and bile duct cannulated Spraque–Dawley rats were purchased from Hilltop Lab Animals, Inc. (Scottdale, PA). Beagle dogs were purchased from Marshall Farms (North Rose, NY).

In Vivo Pharmacokinetics in Rat and Dog. Compound **2** trifluoroacetate salt was administered to groups of three male rats by either IV bolus (1 mg/kg; all doses were **1** equivalent) or oral gavage (5 mg/kg, fasted overnight prior to the dosing). The dosing solution was prepared in PEG-400/ethanol (90/10, v/v) at 1 mg/mL (dosing solution concentration was **1** equivalent) for both IV and oral administration. Plasma samples were collected at intervals up to 24 h and were stored at −20 °C until analysis.

In male beagle dogs (n = 3), the IV and PO studies of **2** were conducted in a crossover fashion. The IV and PO legs were separated by a two-week washout period. In the IV study, **2** hydrochloride salt was infused at 1 mg/kg (equivalent to 0.88 mg/kg **1**) as a solution in water over 5 min. In the oral study, the dogs were fasted overnight before dosing. Prodrug **2** hydrochloride salt was dissolved in water and administered by oral gavage at 5 mg/kg. Plasma samples were collected at intervals up to 24 h and were stored at −20 °C until analysis.

In the oral dose escalation study in rats, **2** trifluoroacetate salt was administered to groups of three male rats by oral gavage at 5, 25, and 200 mg/kg and **1** was given orally at 15, 75, and 200 mg/kg. The dosing solutions were prepared in water with 0.5% methylcellulose.

Pharmacokinetics in Antibiotic-Treated Rats. Two groups of male rats (n = 3, each group) were dosed for 2 days with an antibiotic mixture or saline (control animals). Bacitracin (400 mg/kg BID), neomycin sulfate (400 mg/kg BID), and tetracycline (200 mg/kg) were included in the antibiotic mixture (Watanabe et al.[16]). After antibiotic or saline pretreatment, animals received a 5 mg/kg oral dose of **2**. Plasma samples were collected at intervals up to 24 h and were stored at −20 °C until analysis.

Pharmacokinetics in Dual Cannulated JVC/PVC Rats. Dual cannulated jugular vein cannulated/portal vein cannulated (JVC/PVC) male rats (n = 3) received a 5 mg/kg oral dose of **2**. Plasma samples were collected from the portal vein and the jugular vein up to 24 h and were stored at −20 °C until analysis.

Rat Bile Duct Cannulated Study. Bile duct cannulated/jugular vein cannulated (BDC/JVC) male rats (n = 3) received a 1 mg/kg IV dose of **2**. Plasma, bile, and urine samples were collected up to 6 h. Biotransformation of **2** was evaluated in bile and urine samples. For biotransformation analysis, chromatographic separations were carried out with an HPLC system that consisted of an Accela UPLC (ThermoFisher) and a 3.0 μm Waters Sunfire C-18 (2.1 mm × 150 mm) column maintained at 40 °C. The detectors were an Accela (ThermoFisher) photodiode array detector and an LTQ-Orbitrap Discovery (ThermoFisher) mass spectrometer. The mobile phase, which consisted of 0.1% formic acid in water (A) and acetonitrile (B), was delivered at a flow rate of 0.35 mL/min. A gradient elution program was used for chromatographic separation. The initial mobile phase consisted of 90% solvent A and 10% solvent B, which was held for 2 min, followed by a linear increase to 40% solvent B over 17 min. A step increase to 90% solvent B was employed to wash the column and held for 5 min before returning to the initial conditions. The column was equilibrated for at least 5 min prior to the next injection. The mass spectrometer was operated using an electrospray source in the positive ion mode. Both full scan MS and data dependent MS/MS scanning were used for detection.

In Vitro Incubations. Compound **2** was incubated in Tris-HCl buffer (pH 7.4), rat blood, and rat plasma for 60 min at 37 °C. Incubations were also conducted with commercially available preparations of rat liver cytosol and microsomes as well as human liver microsomes. Aliquots of the cytosol (2 mg/mL) and microsomes (1 mg/mL) were incubated with **2** and 1 mM NADPH for up to 2 h in a shaking water bath at 37 °C. Rat hepatocytes were isolated in-house[15] and were incubated with **2** for 2 h at 37 °C in a humidified incubator with 95/5% air/CO_2.

For anaerobic incubations, rat liver cytosol and microsomes, rat P450 reductase, human liver microsomes, and recombinant human CYP1A2, 2B6, 2D6, 2C8, 2C9, 2C19, and 3A4 were used. Briefly, the incubation buffer (0.1 M phosphate buffer and 10 mM $MgCl_2$) was purged with nitrogen for at least 1 h prior to the start of the incubation and anaerobic incubations were performed under a blanket of humidified nitrogen added directly to sample tubes. Aliquots of the cytosol (2 mg/mL), microsomes (1 mg/mL), recombinant CYPs (made up to 1 mg/mL with the vector control), and P450 reductase (1 mg/mL) were incubated with **2** and 1 mM NADPH for 60 min in a shaking water bath at 37 °C. Finally, prodrugs **2**, **4**, and **5** (40 uM) were incubated in rat feces in LB media (3 g of fresh rat feces suspended in 25 mL of LB media) for 2 h at 37 °C in a shaking water bath.[16] Aliquots were removed and quenched with an equal volume of ice-cold acetonitrile. Following a 10 min centrifugation at ∼1500g, the supernatant was collected and prodrugs and metabolites were detected using LC-UV/MS/MS.

For all in vitro incubations, final substrate (**2**) concentration was 10 μM. At each time point, aliquots of the mixture were removed and immediately quenched with an equal volume of ice-cold acetonitrile. Following a 10 min centrifugation at ∼1500g, the supernatant was collected and **2** and its metabolite (**1**) were quantitated using LC/MS/MS.

LC/MS-MS Analysis of 1 and 2. For quantitation of **1** and **2**, following protein precipitation, supernatants were injected into an API4000 (Applied Biosystems, Foster City, CA) triple quadropole mass spectrometer equipped with a Turboionspray ionization interface operating in the positive ionization mode. The source temperature was 600 °C. The HPLC system used was an Agilent 1200 series (Agilent Technologies, Santa Clara, CA) and a HTC PAL autosampler (Leap Technologies, Cary, NC) linked to a Phenomenex Luna 2.5 um C18-HST analytical column (2.0 mm × 50 mm, 2.5 um; Torrance, CA). The mobile phase, which consisted of 0.1% formic acid in water (A) and 0.1% formic acid in acetonitrile (B), was delivered at a flow rate of 0.6 mL/min. Detection of each analyte was achieved through selected reaction monitoring. Ions representing the precursor $(M + H)^+$ species for **2** and **1** were selected in quadrupole 1 and collisionally dissociated with nitrogen to generate specific product ions, which were subsequently monitored by quadrupole 3. Standard curves defining the dynamic range of the bioanalytical method were prepared in the respective biological matrix and processed in the same fashion as the test samples. Transitions monitored for **2** and **1** were 463.2 → 245.1 and 448.2 → 202.1, respectively. The analysis of **1** and **2** was conducted against a standard curve ranging from 5 to 5000 nM. The standard curve was fitted with a linear regression weighted by the square of the reciprocal concentration $(1/x^2)$.

Pharmacokinetics and Statistical Analysis. Noncompartmental pharmacokinetic analysis of **1** and **2** were performed using Kinetica (Thermo Fisher Scientific, Waltham, MA) from the plasma concentration–time data. Statistical analyses (mean and standard deviation) were performed using Microsoft Excel (Seattle, WA).

AUTHOR INFORMATION

Corresponding Author

*For A.R.R.: phone, 203-677-7416; fax, 203-677-7702; E-mail, alicia.regueiroren@bms.com. For M.S.: phone, 203-677-6646; fax, 203-677-6193; E-mail, michael.sinz@bms.com.

Notes

The authors declare no competing financial interest.

ACKNOWLEDGMENTS

We thank the Pharmaceutical Candidate Optimization Group (Biocon-Bristol Myers Squibb Research Center, Bangalore, India) for conducting the antibiotic treated rat experiment.

ABBREVIATIONS USED

HIV-1, human immunodeficiency virus type 1; AI, attachment inhibitor; BCS, Biopharmaceutics Classification System; BID (bis in die), twice a day; Caco-2, human colorectal adenocarcinoma-2; ppm, parts per million; AUC, area under the plasma concentration–time curve; CYP, cytochrome P450;

DMSO, dimethylsulfoxide; PEG, polyethylene glycol; LB Media, Luria−Bertani media; C_{max}, maximum plasma concentration; Cl, clearance; V_{ss}, volume of distribution; NADPH, β-nicotinamide adenine dinucleotide phosphate reduced tetrasodium salt; BDC, bile-duct cannulated; IV, intravenous; PO, oral; JVC, jugular vein cannulated; PVC, portal vein cannulated; HPLC, high pressure liquid chromatography; LC-MS, liquid chromatography mass spectroscopy; NMR, nuclear magnetic resonance; TMS, trimethylsilane; HRMS, high resolution mass spectrometry; MeOH, methanol; MeCN, acetonitrile; RP-HPLC, reverse phase high pressure liquid chromatography; TFA, trifluoroacetic acid; DMF, dimethylformamide; Rt, retention time; rt, room temperature; min, minutes; h, hours

REFERENCES

(1) Regueiro-Ren, A.; Xue, Q. M.; Swidorski, J. J.; Gong, Y.-F.; Mathew, M.; Parker, D. D.; Yang, Z.; Eggers, B.; D'Arienzo, C.; Sun, Y.; Malinowski, J.; Gao, Q.; Wu, D.; Langley, D. R.; Colonno, R. J.; Chien, C.; Grasela, D. M.; Zheng, M.; Lin, P.-F.; Meanwell, N. A.; Kadow, J. F. Inhibitors of Human Immunodeficiency Virus Type 1 (HIV-1) Attachment 12. Structure−Activity Relationships Associated with 4-Fluoro-6-azaindole Derivatives Leading to the Identification of 1-(4-Benzoyl-piperazin-1-yl)-2-(4-fluoro-7-[1,2,3]triazol-1-yl-1*H*-pyrrolo-[2,3-*c*]pyridin-3-yl)-ethane-1,2-dione (BMS-585248). *J. Med. Chem.* **2013**, DOI: 10.1021/jm3016377.

(2) Kadow, J. F.; Ueda, Y.; Meanwell, N. A.; Connolly, T. P.; Wang, T.; Chen, C.-P.; Yeung, K.-S.; Zhu, J.; Bender, J. A.; Yang, Z.; Parker, D.; Lin, P.-F.; Colonno, R. J.; Mathew, M.; Morgan, D.; Zheng, M.; Chien, C.; Grasela, D. Inhibitors of Human Immunodeficiency Virus Type 1 (HIV-1) Attachment 6. Preclinical and Human Pharmacokinetic Profiling of BMS-663749, a Phosphonooxymethyl Prodrug of the HIV-1 Attachment Inhibitor 2-(4-Benzoyl-1-piperazinyl)-1-(4,7-dimethoxy-1*H*-pyrrolo[2,3-*c*]pyridin-3-yl)-2-oxoethanone (BMS-488043). *J. Med. Chem.* **2012**, *55*, 2048−2056.

(3) Regueiro-Ren, A.; Jenkins, S. M.; Kim, S.; Mosure, K.; Rahematpura, S.; Simmermacher, J., Sinz, M.; Zheng, M.; Johnson, K.; Meanwell, N. A.; Kadow, J. F. Novel ammonium prodrug: synthesis, pharmacokinetics, mechanism of release and scope. Abstracts of Papers, 240th ACS National Meeting and Exposition, Boston, MA, August 22−26, 2010, MEDI-421.

(4) Kadow, J. F.; Regueiro-Ren, A. Aminium salts of 1,2,3-triazoles as prodrugs of drugs including antiviral agents. U.S. Patent US 20060142298, 2006.

(5) Patterson, L H; McKeown, S R; Robson, T.; Gallagher, R.; Raleigh, S M; Orr, S. Antitumor prodrug development using cytochrome P450 (CYP) mediated activation. *Anti-Cancer Drug Des.* **1999**, *14*, 473−486.

(6) Patterson, L. H. Rationale for the use of aliphatic *N*-oxides of cytotoxic anthraquinones as prodrug DNA binding agents: a new class of bioreductive agent. *Cancer Metastasis Rev.* **1993**, *12*, 119−134.

(7) Bottaro, J. C. Stereospecific conversion of olefins into aziridines by *p*-tolylsulfonylhydroxylamine. *J. Chem. Soc., Chem. Commun.* **1980**, 560−561.

(8) Raap, R. Amination of tetrazoles with hydroxylamine-*O*-sulfonic acid: 1-and 2-aminotetrazoles. *Can. J. Chem.* **1969**, *47*, 3677−3681.

(9) Bellettini, J. R.; Olson, E. R.; Teng, M.; Miller, M. J. In *Encyclopedia of Reagents for Organic Synthesis*; Paquette, L. A., Ed.; Wiley: New York, 1995; Vol 3, pp 2189−2190.

(10) Goeptar, A.; Scheerens, H.; Vermeulen, N. Oxygen and Xenobiotic Reductase Activities of Cytochromoe P450. *Crit. Rev. Toxicol.* **1995**, *25* (1), 25−65.

(11) Dahan, A.; Miller, J. M.; Amidon, G. L. Prediction of solubility and permeability class membership: provisional BCS classification of the world's top oral drugs. *AAPS J.* **2009**, *11*, 740−746.

(12) Broccatelli, F.; Cruciani, G.; Benet, L. Z.; Oprea, T. I. BDDCS Class Prediction for New Molecular Entities. *Mol. Pharmaceutics* **2012**, *9*, 570−580.

(13) Sousa, T.; Paterson, R.; Moore, V.; Carlsson, A.; Abrahamsson, B.; Basit, A. The gastrointestinal microbiota as a site for the biotransformation of drugs. *Int. J. Pharm.* **2008**, *363*, 1−25.

(14) Bonjouklian, R.; Dally, R. D.; De Dios, A.; Del Prado C., Miriam F.; Dominguez-Fernandez, C.; Jaramillo Aguado, C.; Lopez de Uralde-Garmendia, B.; Montero Salgado, C.; Shepherd, T. A. Kinase inhibitors. PCT WO 2005080380, 2005.

(15) Berry, M. N., Edwards, A. M., Barritt, G. J. *Laboratory Techniques in Biochemistry and Molecular Biology: Isolated Hepatocytes Preparation, Properties and Applications*; Elsevier: Amsterdam, 1991.

(16) Watanabe, K.; Yamashita, S.; Furuno, K.; Kawasaki, H.; Gomita, Y. Metabolism of omeprazole by gut flora in rats. *J. Pharm. Sci.* **1995**, *84*, 516−517.